



---

RESEARCH ARTICLE

---

INVESTIGATION OF NEUTRON-INDUCED REACTION CROSS SECTIONS FOR  
SEVERAL NUCLEAR REACTOR STRUCTURAL MATERIALS

Murat DAĞ<sup>1,\*</sup> 

<sup>1</sup> Vocational School of Health Services, Kırşehir Ahi Evran University, Kırşehir, Turkey

ABSTRACT

Selection of the appropriate materials as a structural components of nuclear reactor are of key importance to implement the highest efficiency and security. Zr, Fe, Cr, Sn and Nb are commonly used materials involved in structural alloy inside the reactor. The presented result of neutron-induced reaction cross section calculations for  $^{50-52-53-54}\text{Cr}$ ,  $^{54-56-57}\text{Fe}$ ,  $^{93}\text{Nb}$ ,  $^{117}\text{Sn}$ ,  $^{90-91-92}\text{Zr}$  have been computed using Constant Temperature Model, Back Shifted Fermi Gas Model, Generalised Super Fluid Model and Microscopic level densities presented in TALYS 1.9 nuclear code. The calculations have been repeated by changing the level density parameter  $a$  for each isotope and model to observe changes in the model assumption. The obtained results are compared with the experimental data taken from the literature.

**Keywords:** Level density models; Level density parameter; TALYS 1.9, Reactor structural components

---

1. INTRODUCTION

A typical reactor core contains several fuel rods and each of these tubes submerged in following water channels hosts a number of fuel pellets. These fuel tubes help to contain nuclear fuel and fission products while transferring the intense nuclear heat aroused inside the core to the coolant mechanism. Given the fact that the nuclear fuel typically remains for several years and nuclear structural continuously exposed to high temperature, mechanical stress and intense radiation; one of primary concern related to performance and safety of nuclear reactor is substantial changes and degradation in properties of structure material [1].

The choice of structural materials using as a containment of fuel and fission products inside nuclear reactor core are therefore the essential factor needed to be meticulously considered. By providing good high temperature strength, increased corrosion and especially neutron radiation damage resistance; the durability of this component subjected to intense fluxes of high-energy neutrons along with excessive thermo-mechanical stresses can be improved. In most commercial reactors, due to the adequate corrosion performance and large neutron cross sections, zirconium-based alloy systems are used. Contrary to other alloy systems, the corrosion performance of zirconium alloy initially boosted by adding almost any alloying elements compared to the less contaminated alloy. Furthermore, it was found that a very small proportion (typically less than 0.5%) of alloying element additions is sufficient enough to effect significant changes in corrosion behavior on zirconium alloy system. In the light of the discovery of this unusual feature of the zirconium alloy, a systematic search for alloying elements that enhanced both corrosion resistance and mechanical properties began without eliminating large neutron cross sections [2].

Two main alloy systems were thus considered to develop for use in the cores of nuclear reactors: a zirconium-tin-based system (Zircoloy family) and a Zirconium-Niobium system. Zircoloy-family gave

rise in the United States, whereas a Zirconium-Niobium system in other countries such as Russia and Canada. Zircolay-1 (Zr-1.5% Sn), after performed reasonably well, was then improved by adding 0.15%Fe, 0.10% Cr, 0.05% Ni and named Zircolay-2. Zircaloy-2 has been predominantly used in Boiling Water Reactors (BWR), while in PWR Zircaloy-4 (Zr-1.5%Sn-0.2%Fe-0.1%Cr) typically used in Pressurized Water Reactors (PWR) and CANDU reactor. In Russian reactors VVERs (similar to PWRs) E110 alloy was used, whereas Zircolay-4 was preferred to use in PWR plants. E110 alloy was a binary Zr-1%Nb alloy. Another type alloy used in Russian VVER application was E635, which both contained both Sn and Nb [2]. Besides, recent developments tend to increase iron content in Zirconium alloy systems [3].

Calculating neutron-induced reaction cross sections of Zr-Fe-Cr-Sn-Nb element therefore gives some insight into the suite of alloys that used in the structural and provides a degree of information regarding the role of insulation and resistance of zirconium alloy to the harmful effects of radiation. For that purpose, previously studies for calculation of the cross sections of the various interested reaction are done with help of available codes such as TALYS, EMPIRE, ALICE which include theoretical models developed by the combination of exist theoretical knowledge and previously obtained outcomes of the experiments [4-7].

## 2. MATERIAL AND METHOD

TALYS, a scientific computer code, has a wide range of use in the analysis and prediction of nuclear reactions. The principle of its operation is basically to simulate the nuclear reaction, where the light particle in energy range of 1 keV – 200 MeV interacts with the target nuclide of mass heavier than 12, by means of a suite of nuclear reaction model, and give us insight in the fundamental interaction between particles and nuclei, and precise measurements enable us to review and correct the theoretical models [8, 9].

The measurement of the relative probability for the reaction to occur is called cross section, and having the knowledge of cross section data is obligatory in order to assume nuclear reaction patterns and channels. However, due to the insufficient data available, it is a key issue to have the knowledge of cross section of a particular reaction. Therefore, at the energies of interest in which discrete level information is missing or incomplete, nuclear level densities are used in order to predict cross sections using statistical model.

Three level density models, Constant Temperature Model (CTM) [10], Back-Shifted Fermi Gas Model (BSFGM) [11–13], Generalized Superfluid Model (GSM) [9, 14] and Microscopic Level Densities (MLD), are widely used in practical calculations of nuclear level densities, and these three level density models have been reviewed in TALYS.

Level densities, as mentioned above, one of key elements in investigation of nuclear reaction cross section, and the theoretical model calculations have a primary role to play in determining the accuracy of parameters in the model and experimental data. Therefore, calculating the level density parameters for isotopes is helpful in investigating the cross section of the reaction of interest.

It was proposed that the level density parameter  $a$  is a nuclide-specific constant and treated as an independent parameter on energy for an entire range of nuclide [10, 13, 15]. It was later [14] recognized the correlation between the level density parameter and the shell correction term of the liquid-drop component of the mass formula. To obtain the more realistic level density, it was assumed that the Fermi Gas formula is still valid but the parameter  $a$  is as a dependent parameter on energy and shown as following.

$$a = a(E_x) = \tilde{a} \left( 1 + \delta W \frac{[1 + \exp[-\gamma U]]}{U} \right), \quad (1)$$

with  $U$ , the effective excitation energy, which is defined by  $U = E_x - \Delta$ , denote the true excitation energy and the energy shift, respectively.  $\gamma$ , the damping parameter, determines how rapidly  $a(E_x)$  approaches  $\tilde{a}$ , the asymptotic level density value.  $\delta W$  is the shell correction energy.

There are also microscopic approaches besides the phenomenological models presented in TALYS. In this approaches, level density calculation has been calculated by S. Goriely on the basis of Hartree-Fock calculation. New energy, spin and parity dependent nuclear level densities based on the microscopic combinatorial model was proposed by Hillaire and Goriely [16]. The most recent option in microscopic approaches has been included in this study, which is based on temperature-dependent Hartree-Fock-Bogolyubov calculations [17,18].

With these different level density models included in TALYS 1.9, the calculation of neutron-induced reaction cross-sections for each selected isotope of Zr, Fe, Cr, Sn and Nb has been calculated. For each isotope, the first step was to use the default value of the level density parameter ( $a$ ) on each level density model so as to determine the compatibility between the experimental data obtained from the literature in EXFOR and theoretical calculations. The adjustment of value of level density parameter was the next step in order to minimize the conflict between the experimental data and the theoretical predictions as well as find the optimum result. Therefore, chi-square statistic (see Eq. 2) was used to evaluate differences between the experimental data and the models estimation. The results were compared with the data and shown in graph for each isotope along with table indicating the default and the best value of the level density parameter.

$$\chi^2 = \sum_{i=1}^k \frac{(x_i - m_i)^2}{m_i}, \quad (2)$$

where  $x$  and  $m$  demonstrate the observed and expected value, respectively.

### 3. RESULTS

Theoretical calculations of the reaction  $^{50}\text{Cr}(n,2n)$ ,  $^{50}\text{Cr}(n,3n)$ ,  $^{52}\text{Cr}(n,2n)$ ,  $^{52}\text{Cr}(n,p)$ ,  $^{53}\text{Cr}(n,p)$  and  $^{54}\text{Cr}(n,p)$  using the 4 models are shown in Fig. 1-6. Unlike MLD model the assumption of all 3 models (CTM, BSFGM, GSM) for all 4 isotopes of Chromium using the best value of level density parameter fit well with the literature data to a certain extent. However, MLD model assumption for this reaction cross section always shows a slight divergence from the data points.

As for the reaction  $^{54}\text{Fe}(n,2n)$ ,  $^{54}\text{Fe}(n,p)$ ,  $^{56}\text{Fe}(n,2n)$ ,  $^{56}\text{Fe}(n,p)$  and  $^{57}\text{Fe}(n,p)$  in Fig 7-11, all 3 models (CTM, BSFGM, GSM) show a good agreement with the experimental results. Yet, MLD model assumption is still was not consistent with the experimental results, except for the reaction  $^{56}\text{Fe}(n,2n)$  seen Fig. 9.

Fig. 12-14 show the calculations of the reaction  $^{93}\text{Nb}(n,2n)$ ,  $^{93}\text{Nb}(n,3n)$  and  $^{117}\text{Sn}(n,p)$ . Reaction cross-section estimations for all 4 models are matched, with error within limits. Only MLD model assumption for the reaction  $^{93}\text{Nb}(n,3n)$  is lower than the data points as seen in Fig. 13.

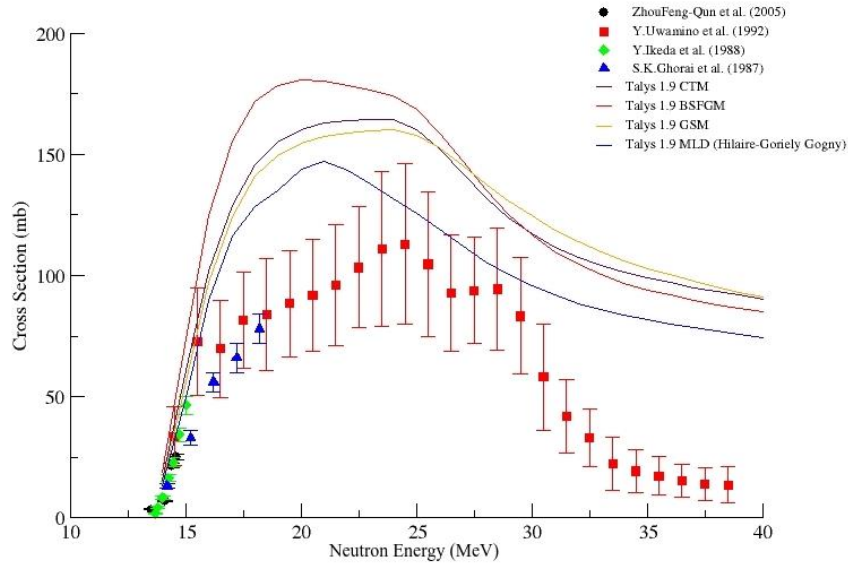
Through Fig. 15-18, the reaction  $^{90}\text{Zr}(n,2n)$ ,  $^{90}\text{Zr}(n,p)$ ,  $^{91}\text{Zr}(n,p)$  and  $^{92}\text{Zr}(n,p)$  are presented. The data and CTM and BSFGM model prediction for  $^{90}\text{Zr}(n,2n)$  and CTM, BSFGM and GSM model for  $^{90}\text{Zr}(n,p)$  are in a good agreement up to 15 MeV. On the contrary, MLD prediction is much lower than the data points. For  $^{91}\text{Zr}(n,p)$  and  $^{92}\text{Zr}(n,p)$ , the model assumptions are well-matched with the experimental results, except MLD for  $^{91}\text{Zr}(n,p)$  is not compatible with the data points.

All 4 model calculations have been done using both the default and best value of level density parameter. It needs to indicate that MLD model prediction for the reaction cross-section has not affected by changing the level density parameters as much as the other models do, therefore the default value for MLD model has keep stable throughout the article. The most compatible theoretical calculation for all 3 models (CTM, BSFGM, GSM) with experimental data points have been presented

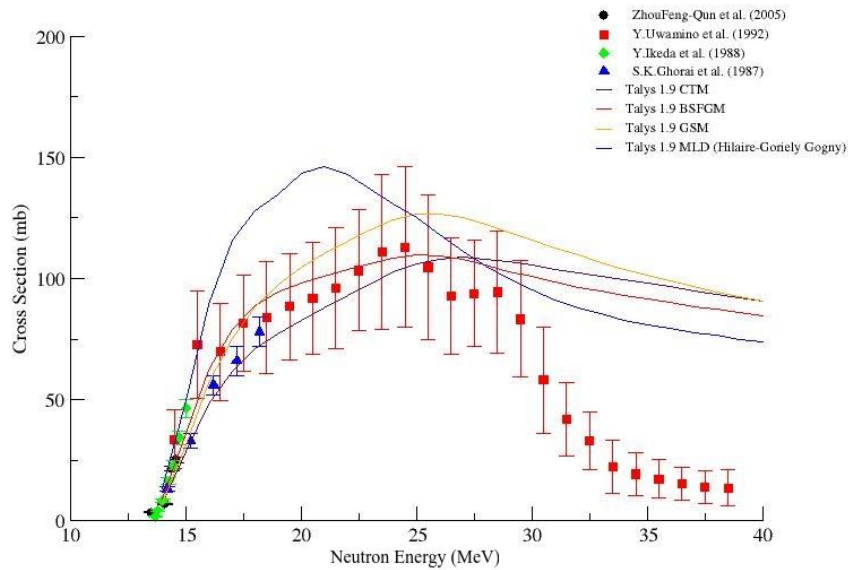
on the same graph to be easily compared with both each other and data points. Also in order to increase the readability, each model is presented its own color in every graph.

#### **4. CONCLUSION**

Today's reactor needs to have high resistance to radiation damage in a manner of material along with having good corrosion resistance. Selection of appropriate materials is, therefore, a challenging issue which arises in this domain. Two main alloy systems, a Zr-Sn and a Zr-Nb system, have been widely adopted; however, it may lead another issue needed to be addressed, the choice of the elements included in alloy systems used as structural materials because, no matter how small portion added the alloy systems, investigation of the characteristic of any alloying elements can prevent myriad problems we may encounter. Hence, neutron-induced reaction cross section of the different isotopes of Zr, Fe, Cr, Sn and Nb contained in structural materials has been investigated by means of 4 level density models (Constant Temperature Model, Back Shifted Fermi Gas Model, Generalised Super Fluid Model and Microscopic level densities) presented in TALYS 1.9 code and compared with literature experimental data. All analyses in this study can help to highlight the success of the model assumption, represent the changes caused by the level density parameter, and most importantly to contribute to the optimization of the models for the future research.



(a)

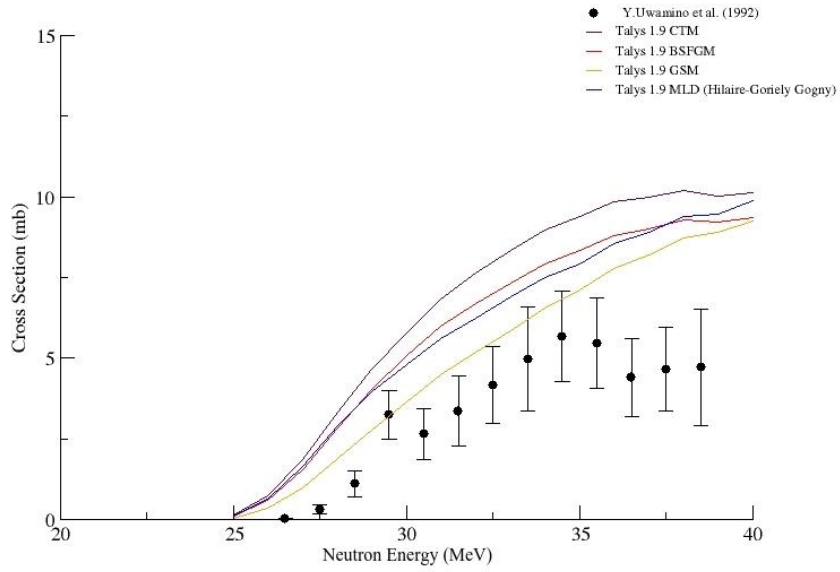


(b)

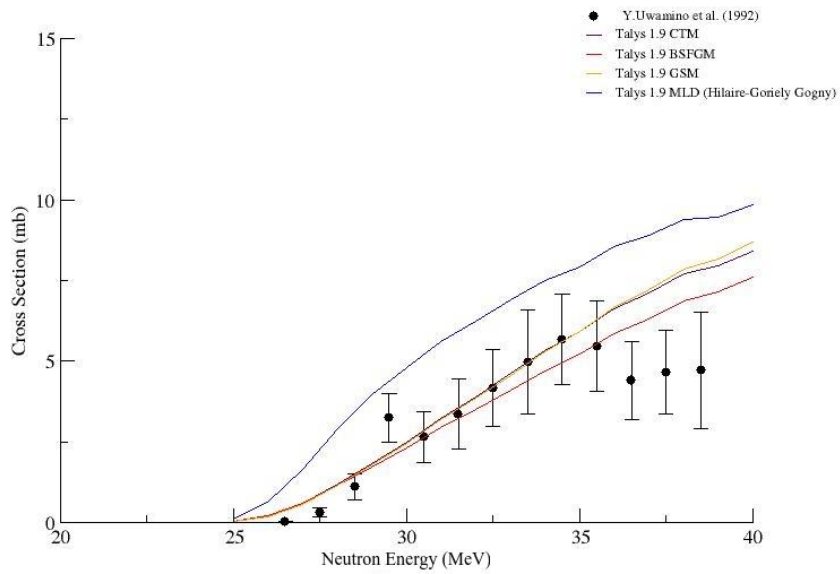
**Figure 1.** The assumptions of all 4 models for the cross-section of the reaction  $^{50}\text{Cr}(n,2n)$  calculated using (a) the default value and (b) the best value of level density parameter value, and compared with the experimental data obtained from EXFOR (<https://www-nds.iaea.org>).

**Table 1.** The default and best value of level density parameter for the reaction  $^{50}\text{Cr}(n,2n)$ .

$^{50}\text{Cr}(n,2n)$	CTM	BSFGM	GSM	MLD
Default	6.67273	5.81303	5.46889	6.67273
Best Fit	5.33818	4.65042	4.37511	6.67273



(a)

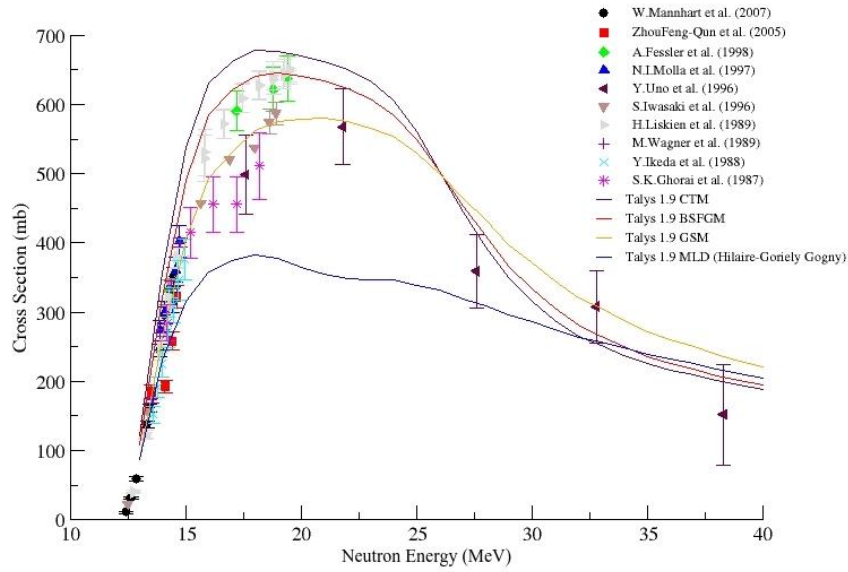


(b)

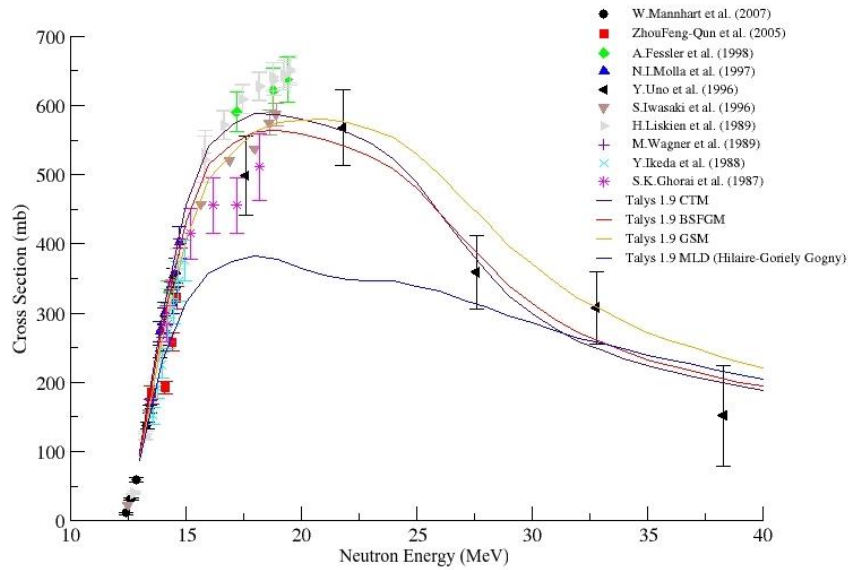
**Figure 2.** The assumptions of all 4 models for the cross-section of the reaction  $^{50}\text{Cr}(n,3n)$  calculated using (a) the default value and (b) the best value of level density parameter value, and compared with the experimental data obtained from EXFOR (<https://www-nds.iaea.org>).

**Table 2.** The default and best value of level density parameter for the reaction  $^{50}\text{Cr}(n,3n)$ .

$^{50}\text{Cr}(n,3n)$	CTM	BSFGM	GSM	MLD
<b>Default</b>	6.67273	5.81303	5.46889	6.67273
<b>Best Fit</b>	5.33818	4.65042	4.37511	6.67273



(a)



(b)

**Figure 3.** The assumptions of all 4 models for the cross-section of the reaction  $^{52}\text{Cr}(n,2n)$  calculated using (a) the default value and (b) the best value of level density parameter value, and compared with the experimental data obtained from EXFOR (<https://www-nds.iaea.org>).

**Table 3.** The default and best value of level density parameter for the reaction  $^{52}\text{Cr}(n,2n)$ .

$^{52}\text{Cr}(n,2n)$	CTM	BSFGM	GSM	MLD
Default	6.81196	5.92668	5.57222	6.81196
Best Fit	6.13076	5.33401	5.57222	6.81196

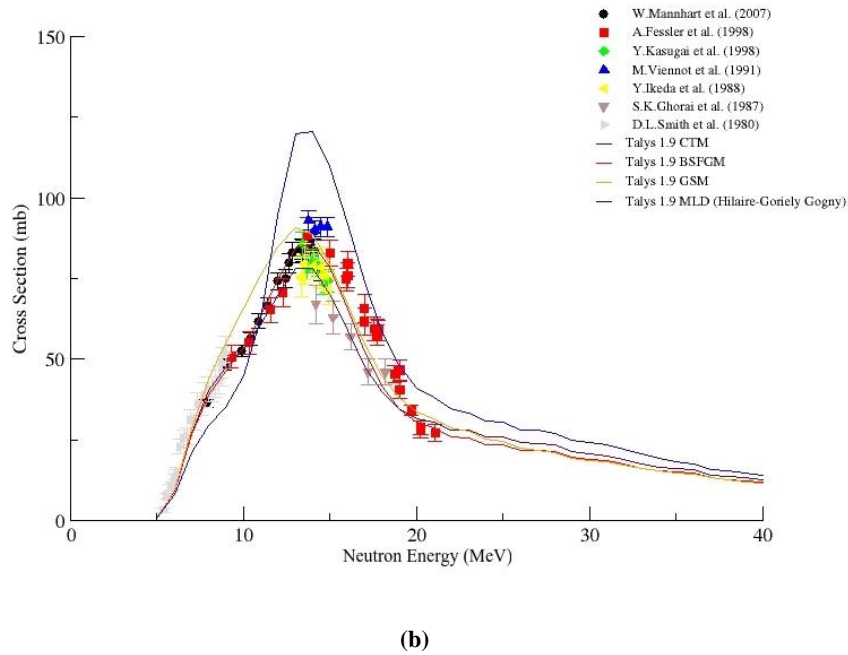
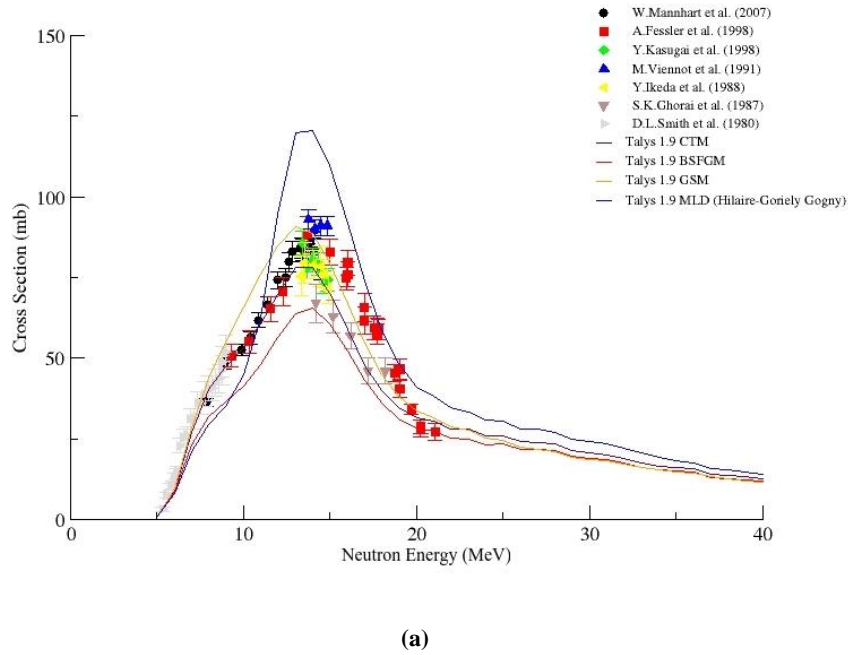
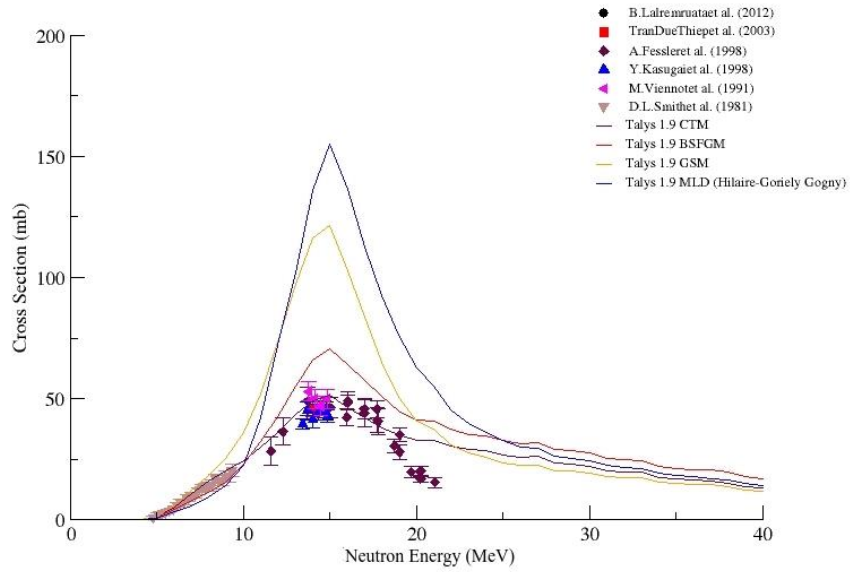


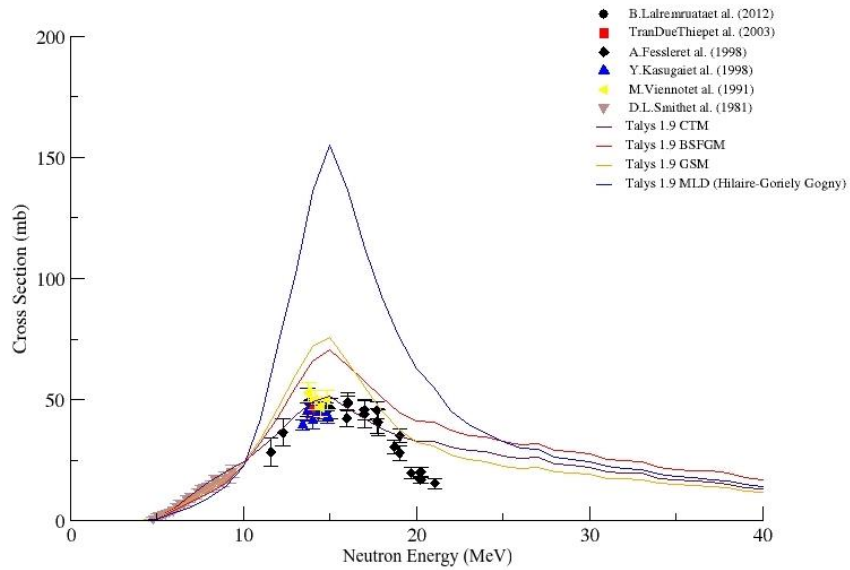
**Figure 4.** The assumptions of all 4 models for the cross-section of the reaction  $^{52}\text{Cr}(n,p)$  calculated using (a) the default value and (b) the best value of level density parameter value, and compared with the experimental data obtained from EXFOR (<https://www-nds.iaea.org>).

**Table 4.** The default and best value of level density parameter for the reaction  $^{52}\text{Cr}(n,p)$ .

$^{52}\text{Cr}(n,p)$	CTM	BSFGM	GSM	MLD
Default	6.81196	5.92668	5.57222	6.81196
Best Fit	6.81196	5.63034	5.57222	6.81196



(a)



(b)

**Figure 5.** The assumptions of all 4 models for the cross-section of the reaction  $^{53}\text{Cr}(n,p)$  calculated using (a) the default value and (b) the best value of level density parameter value, and compared with the experimental data obtained from EXFOR (<https://www-nds.iaea.org>).

**Table 5.** The default and best value of level density parameter for the reaction  $^{53}\text{Cr}(n,p)$ .

$^{53}\text{Cr}(n,p)$	CTM	BSFGM	GSM	MLD
Default	6.45133	5.20851	5.08128	6.94579
Best Fit	6.45133	5.20851	5.58940	6.94579

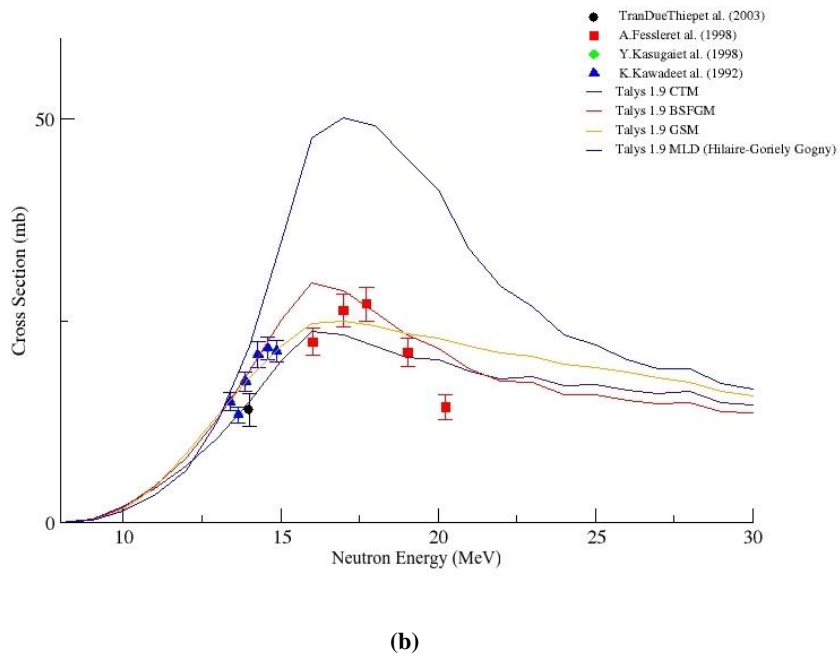
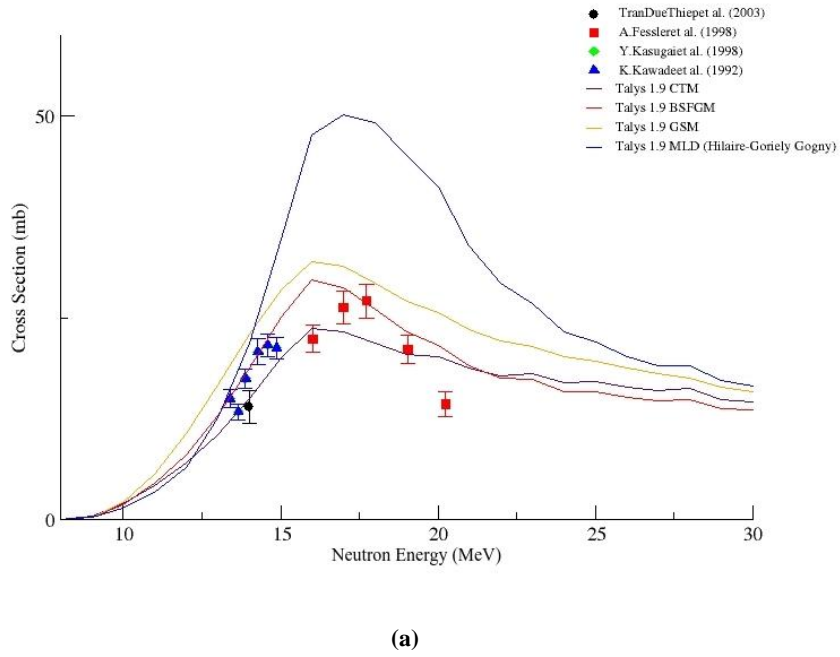
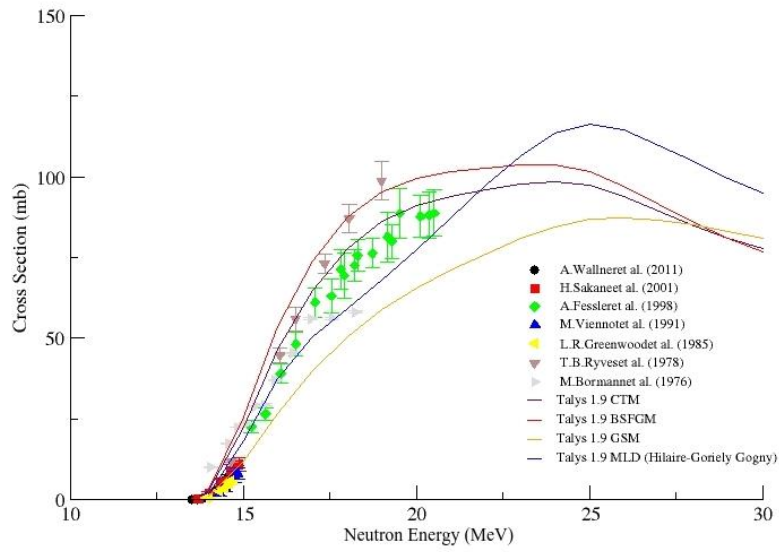


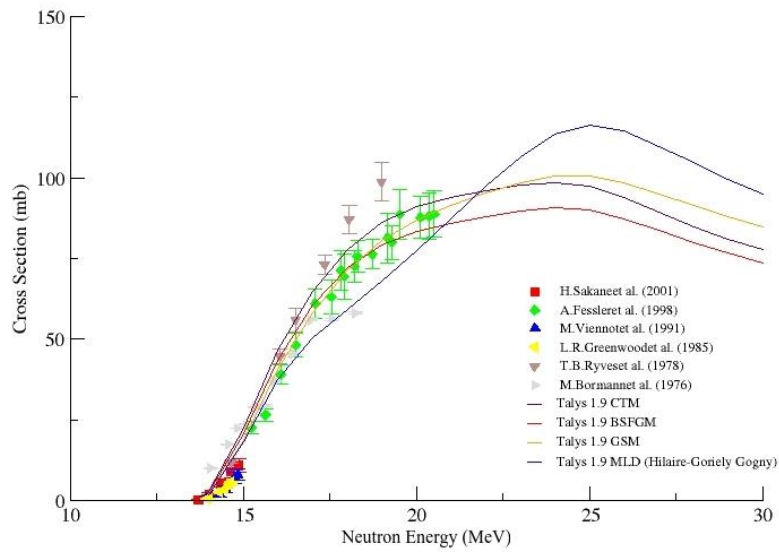
**Figure 6.** The assumptions of all 4 models for the cross-section of the reaction  $^{54}\text{Cr}(n,p)$  calculated using (a) the default value and (b) the best value of level density parameter value, and compared with the experimental data obtained from EXFOR (<https://www-nds.iaea.org>).

**Table 6.** The default and best value of level density parameter for the reaction  $^{54}\text{Cr}(n,p)$ .

$^{54}\text{Cr}(n,p)$	CTM	BSFGM	GSM	MLD
Default	6.94365	5.43819	5.34845	7.5843
Best Fit	6.94365	5.43819	5.88329	7.5843



(a)

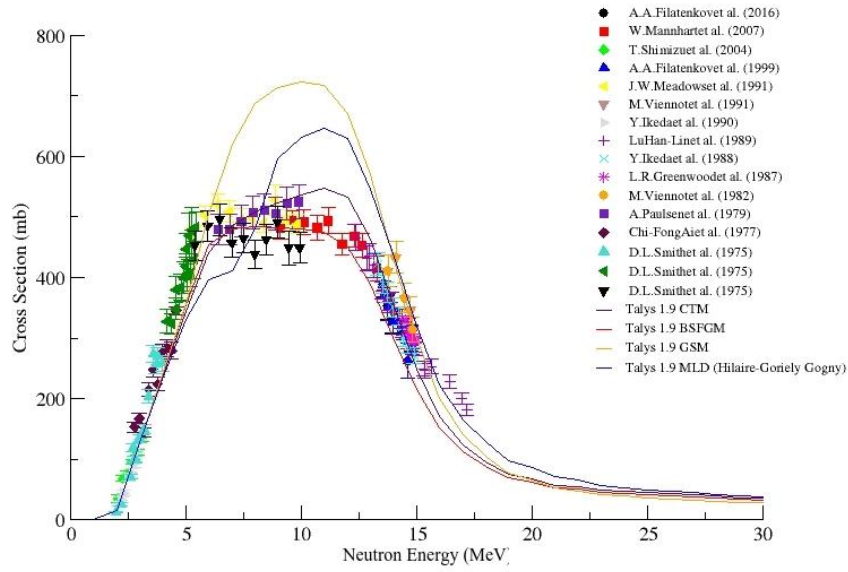


(b)

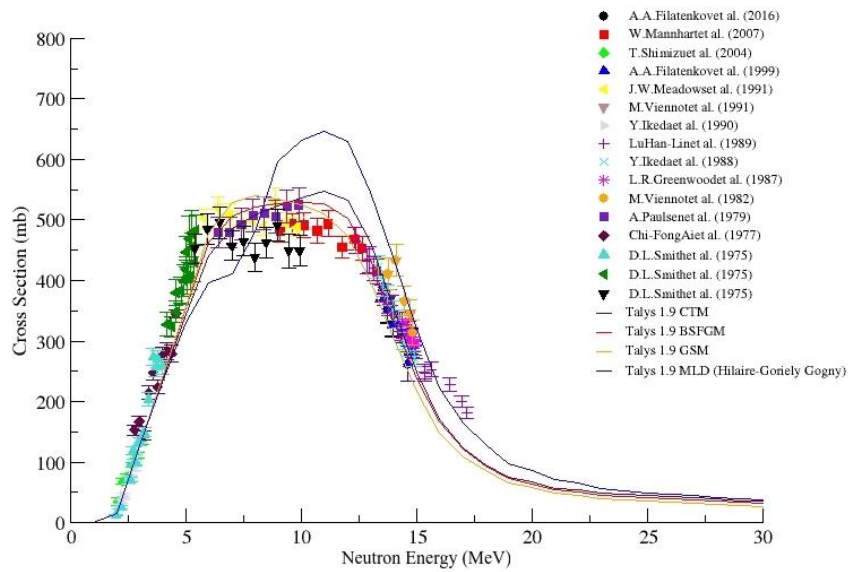
**Figure 7.** The assumptions of all 4 models for the cross-section of the reaction  $^{54}\text{Fe}(n,2n)$  calculated using (a) the default value and (b) the best value of level density parameter value, and compared with the experimental data obtained from EXFOR (<https://www-nds.iaea.org>).

**Table 7.** The default and best value of level density parameter for the reaction  $^{54}\text{Fe}(n,2n)$ .

$^{54}\text{Fe}(n,2n)$	CTM	BSFGM	GSM	MLD
Default	6.00039	5.38875	5.02767	6.00039
Best Fit	6.00039	5.119312	5.781820	6.00039



(a)

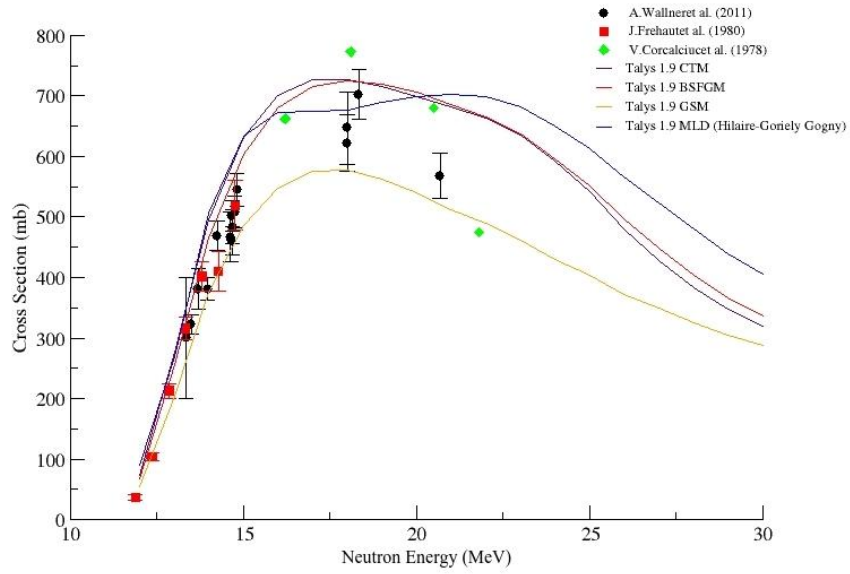


(b)

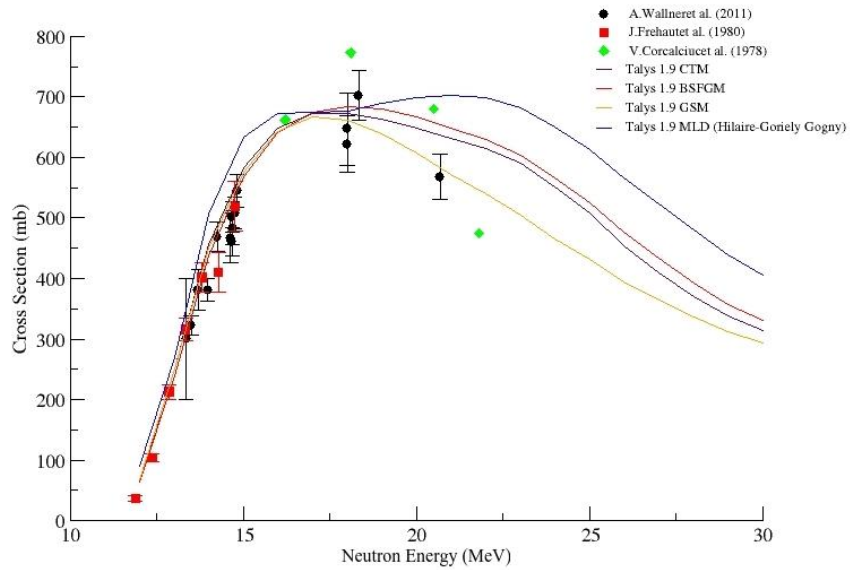
**Figure 8.** The assumptions of all 4 models for the cross-section of the reaction  $^{54}\text{Fe}(n,p)$  calculated using (a) the default value and (b) the best value of level density parameter value, and compared with the experimental data obtained from EXFOR (<https://www-nds.iaea.org>).

**Table 8.** The default and best value of level density parameter for the reaction  $^{54}\text{Fe}(n,p)$ .

$^{54}\text{Fe}(n,p)$	CTM	BSFGM	GSM	MLD
Default	6.00039	5.38875	5.02767	6.00039
Best Fit	6.00039	5.227087	6.03320	6.00039



(a)

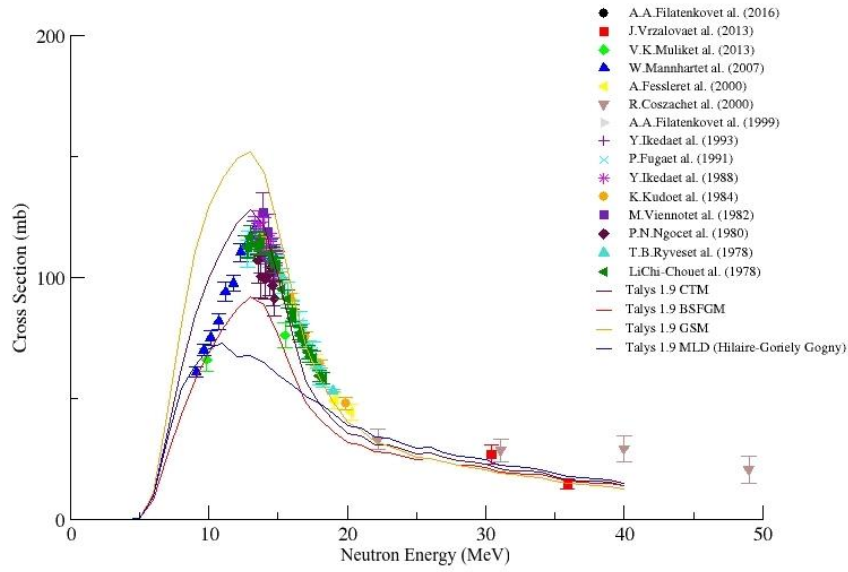


(b)

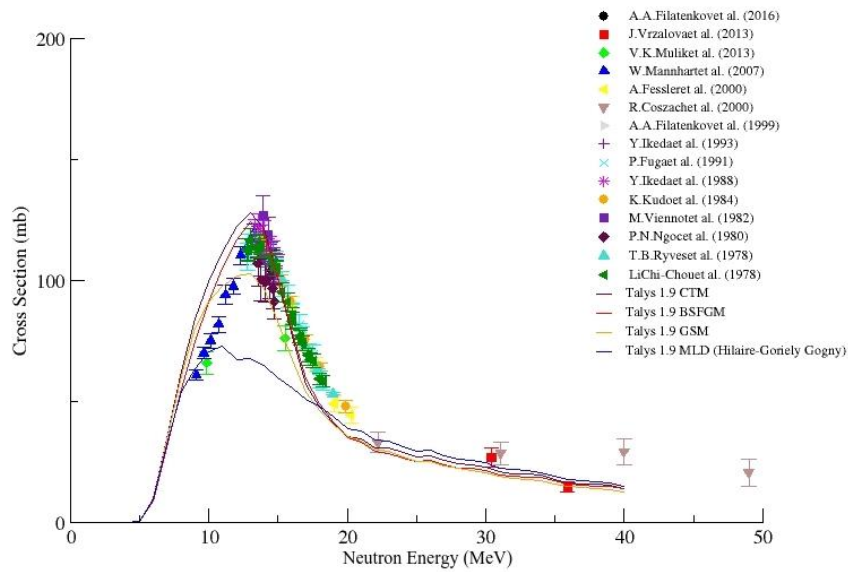
**Figure 9.** The assumptions of all 4 models for the cross-section of the reaction  $^{56}\text{Fe}(n,2n)$  calculated using (a) the default value and (b) the best value of level density parameter value, and compared with the experimental data obtained from EXFOR (<https://www-nds.iaea.org>).

**Table 9.** The default and best value of level density parameter for the reaction  $^{56}\text{Fe}(n,2n)$ .

$^{56}\text{Fe}(n,2n)$	CTM	BSFGM	GSM	MLD
Default	6.73168	5.96126	5.58624	6.73168
Best Fit	6.39509	5.66319	6.70348	6.73168



(a)



(b)

**Figure 10.** The assumptions of all 4 models for the cross-section of the reaction  $^{56}\text{Fe}(n,p)$  calculated using (a) the default value and (b) the best value of level density parameter value, and compared with the experimental data obtained from EXFOR (<https://www-nds.iaea.org>).

**Table 10.** The default and best value of level density parameter for the reaction  $^{56}\text{Fe}(n,p)$ .

$^{56}\text{Fe}(n,p)$	CTM	BSFGM	GSM	MLD
Default	6.73168	5.96126	5.58624	6.73168
Best Fit	6.73168	5.66319	6.14486	6.73168

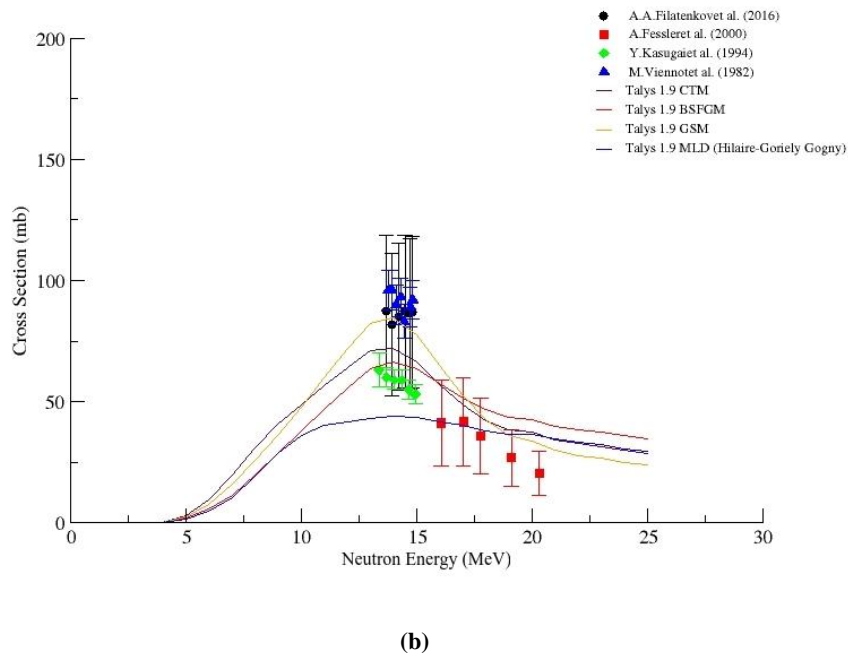
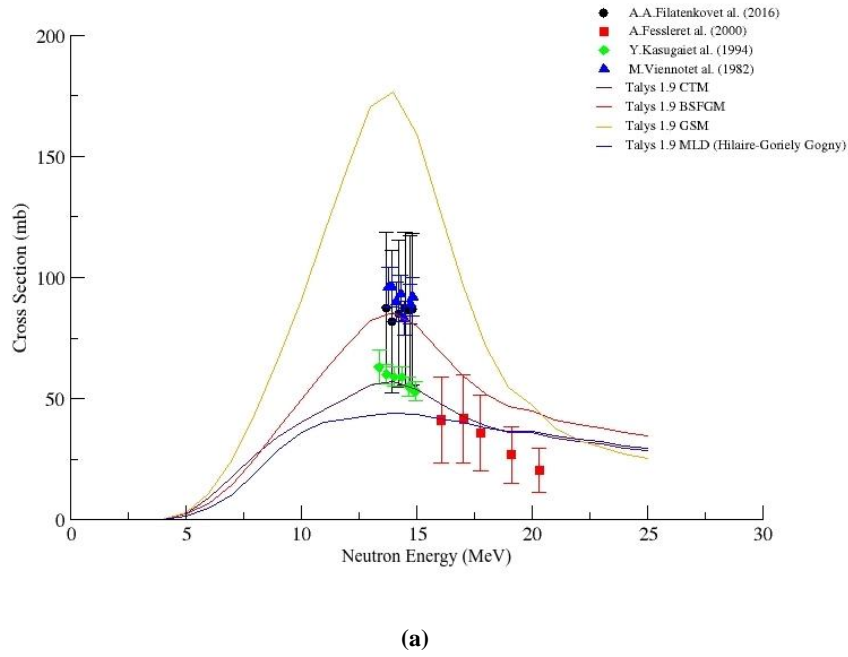
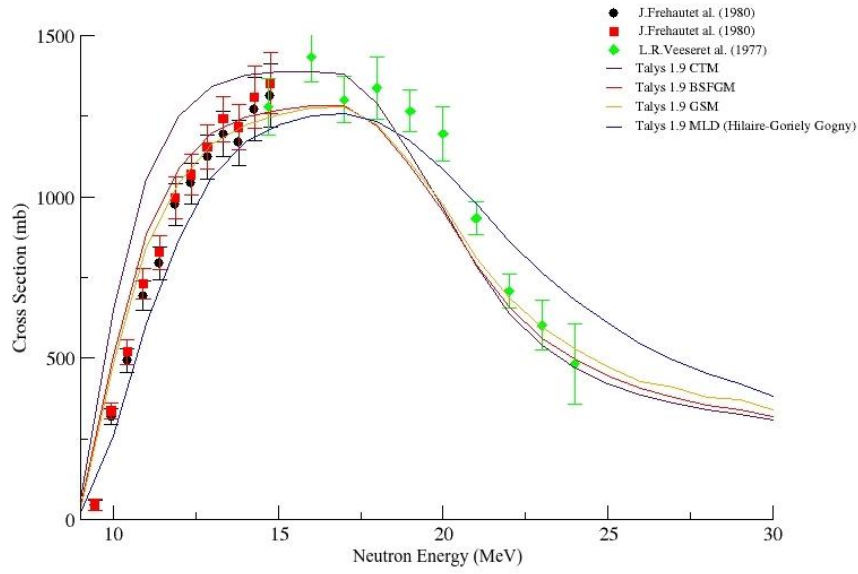


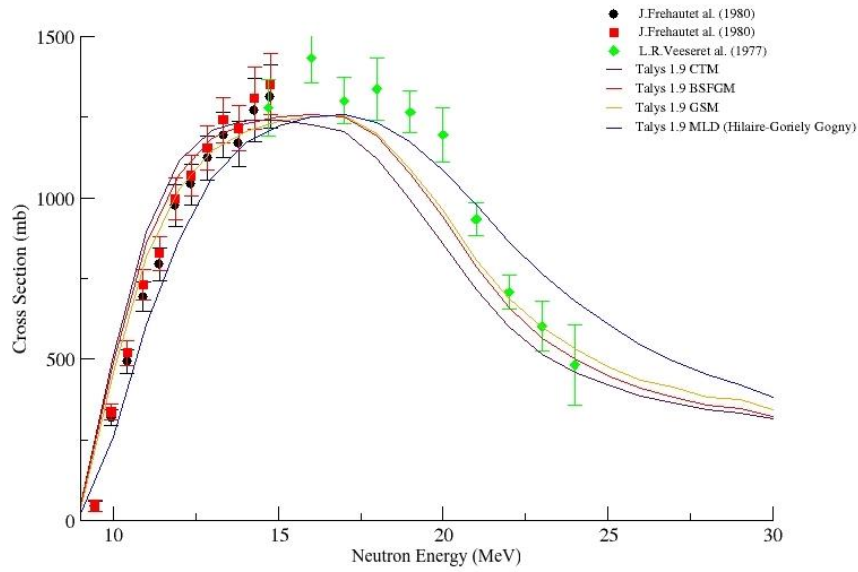
**Figure 11.** The assumptions of all 4 models for the cross-section of the reaction  $^{57}\text{Fe}(n,p)$  calculated using (a) the default value and (b) the best value of level density parameter value, and compared with the experimental data obtained from EXFOR (<https://www-nds.iaea.org>).

**Table 11.** The default and best value of level density parameter for the reaction  $^{57}\text{Fe}(n,p)$ .

$^{57}\text{Fe}(n,p)$	CTM	BSFGM	GSM	MLD
Default	7.21045	6.25324	5.89597	7.26476
Best Fit	6.84992	6.56590	6.78036	7.26476



(a)

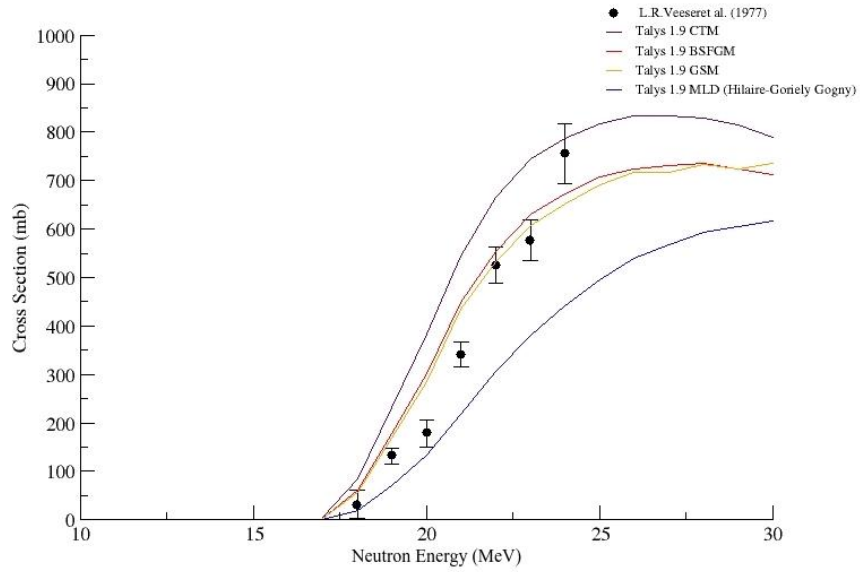


(b)

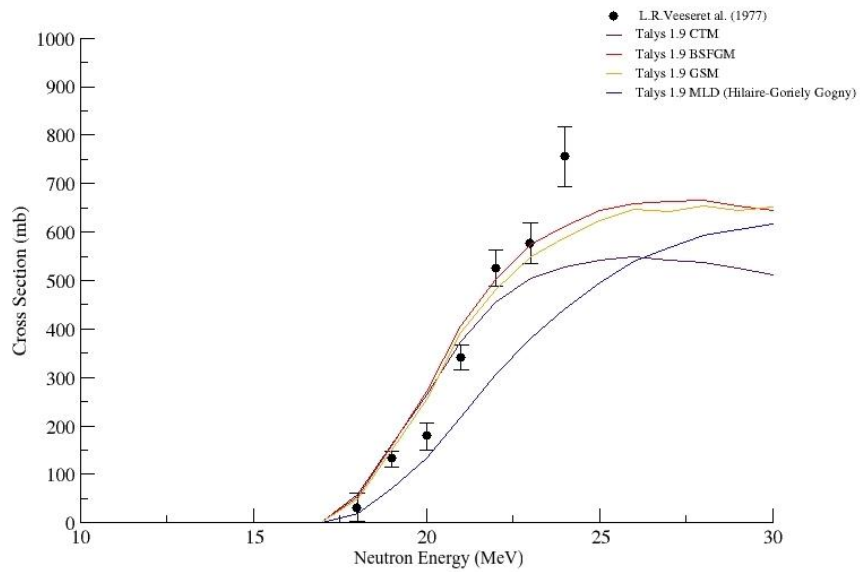
**Figure 12.** The assumptions of all 4 models for the cross-section of the reaction  $^{93}\text{Nb}(n,2n)$  calculated using (a) the default value and (b) the best value of level density parameter value, and compared with the experimental data obtained from EXFOR (<https://www-nds.iaea.org>).

**Table 12.** The default and best value of level density parameter for the reaction  $^{93}\text{Nb}(n,2n)$ .

$^{93}\text{Nb}(n,2n)$	CTM	BSFGM	GSM	MLD
Default	12.33156	10.79489	11.01774	12.33156
Best Fit	9.86524	9.71540	9.91596	12.33156



(a)



(b)

**Figure 13.** The assumptions of all 4 models for the cross-section of the reaction  $^{93}\text{Nb}(n,3n)$  calculated using (a) the default value and (b) the best value of level density parameter value, and compared with the experimental data obtained from EXFOR (<https://www-nds.iaea.org>).

**Table 13.** The default and best value of level density parameter for the reaction  $^{93}\text{Nb}(n,3n)$ .

$^{93}\text{Nb}(n,3n)$	CTM	BSFGM	GSM	MLD
Default	12.33156	10.79489	11.01774	12.33156
Best Fit	9.86524	9.71540	9.91596	12.33156

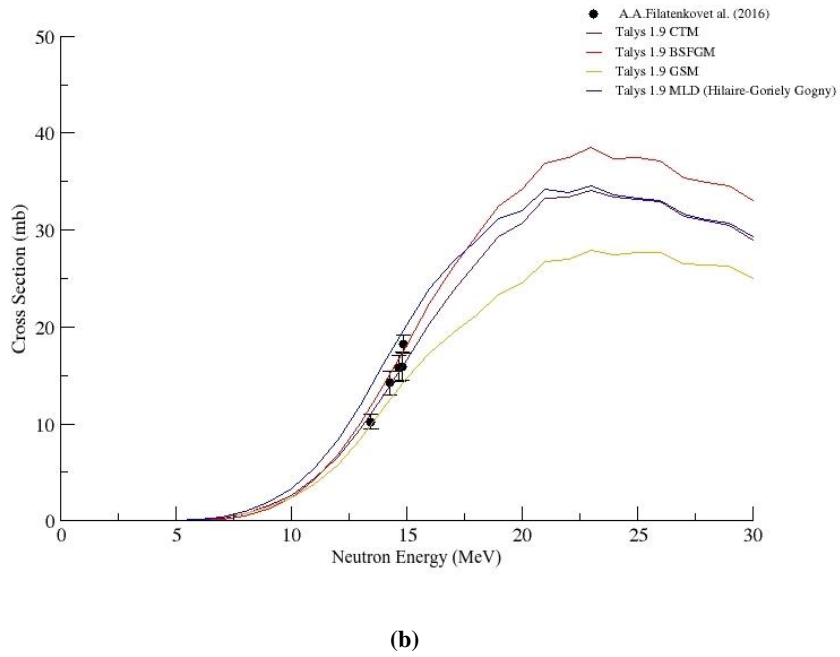
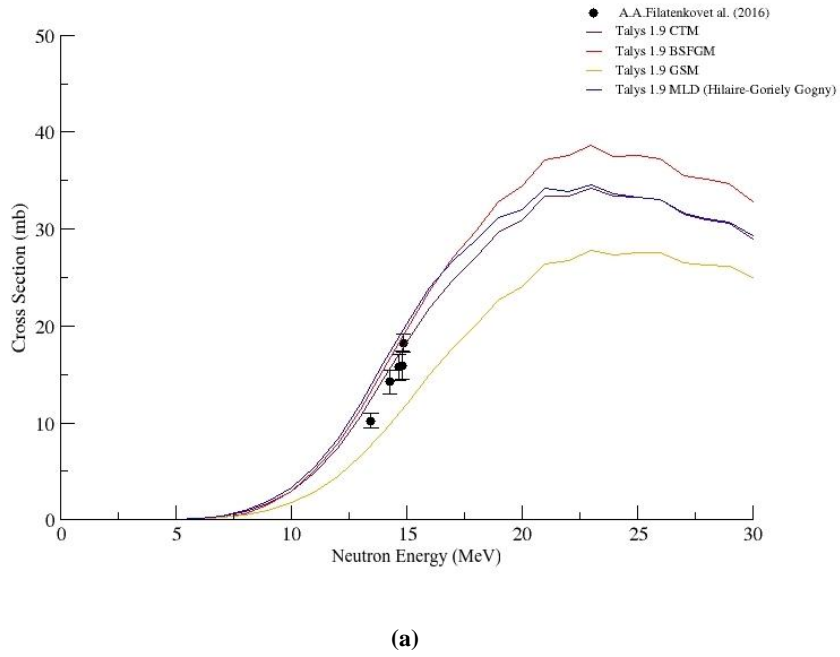
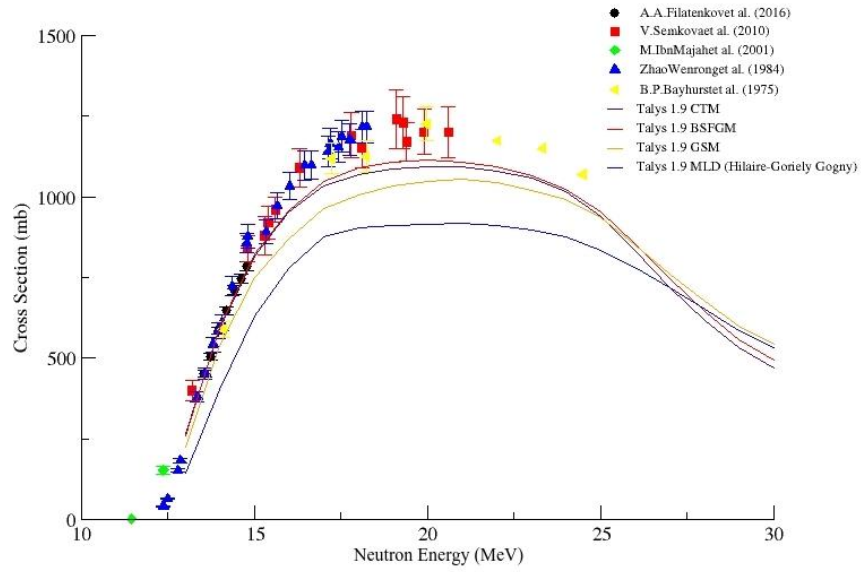


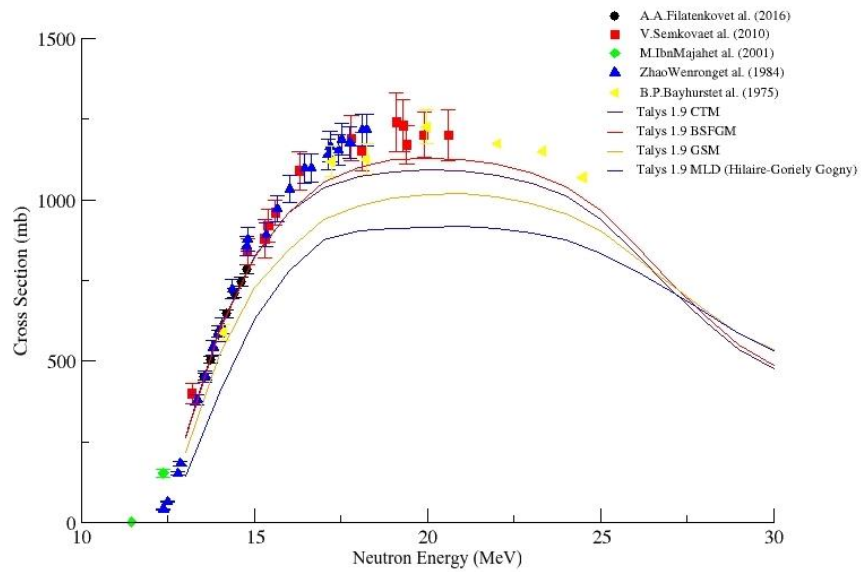
**Figure 14.** The assumptions of all 4 models for the cross-section of the reaction  $^{117}\text{Sn}(n,p)$  calculated using (a) the default value and (b) the best value of level density parameter value, and compared with the experimental data obtained from EXFOR (<https://www-nds.iaea.org>).

**Table 14.** The default and best value of level density parameter for the reaction  $^{117}\text{Sn}(n,p)$ .

$^{117}\text{Sn}(n,p)$	CTM	BSFGM	GSM	MLD
<b>Default</b>	15.84277	15.33552	17.14004	16.35188
<b>Best Fit</b>	17.42704	18.40262	13.71203	16.35188



(a)



(b)

**Figure 15.** The assumptions of all 4 models for the cross-section of the reaction  $^{90}\text{Zr}(n,2n)$  calculated using (a) the default value and (b) the best value of level density parameter value, and compared with the experimental data obtained from EXFOR (<https://www-nds.iaea.org>).

**Table 15.** The default and best value of level density parameter for the reaction  $^{90}\text{Zr}(n,2n)$ .

$^{90}\text{Zr}(n,2n)$	CTM	BSFGM	GSM	MLD
Default	10.43527	9.18676	9.00435	10.43527
Best Fit	9.91350	10.10543	8.55413	10.43527

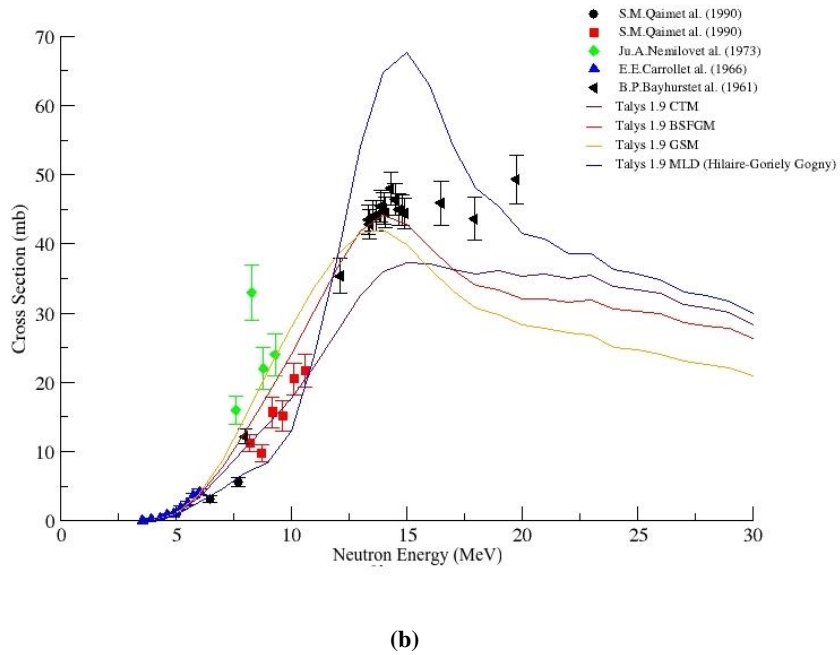
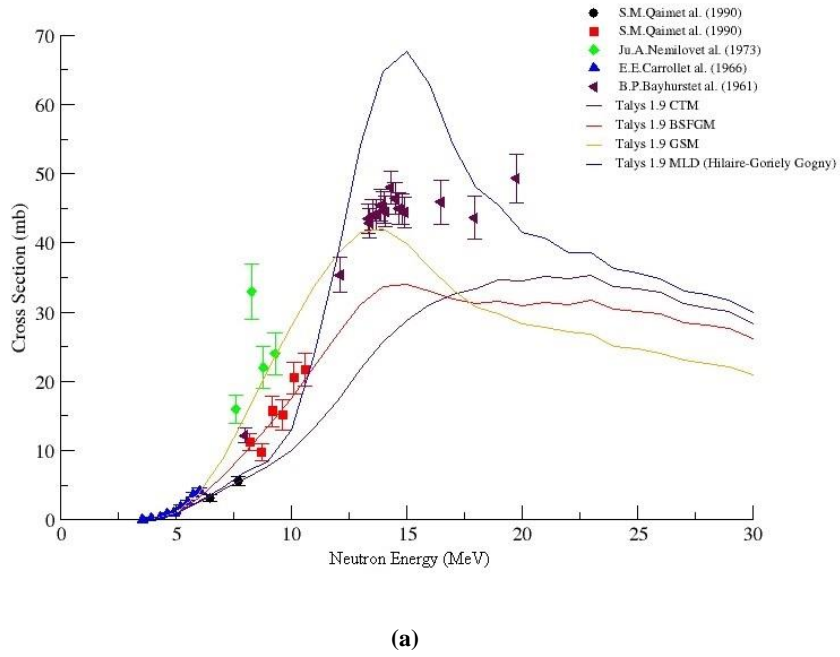
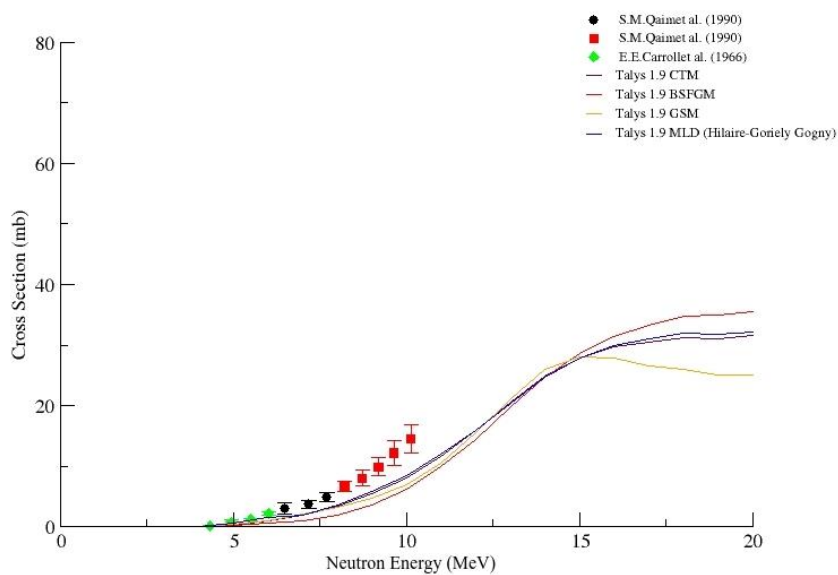


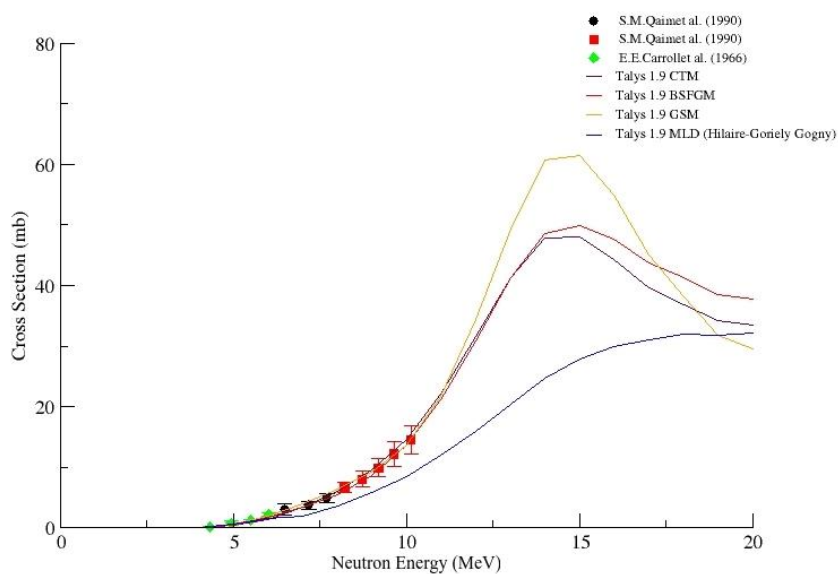
**Figure 16.** The assumptions of all 4 models for the cross-section of the reaction  $^{90}\text{Zr}(n,p)$  calculated using (a) the default value and (b) the best value of level density parameter value, and compared with the experimental data obtained from EXFOR (<https://www-nds.iaea.org>).

**Table 16.** The default and best value of level density parameter for the reaction  $^{90}\text{Zr}(n,p)$ .

$^{90}\text{Zr}(n,p)$	CTM	BSFGM	GSM	MLD
Default	10.43527	9.18676	9.00435	10.43527
Best Fit	9.39174	8.72742	9.00435	10.43527



(a)

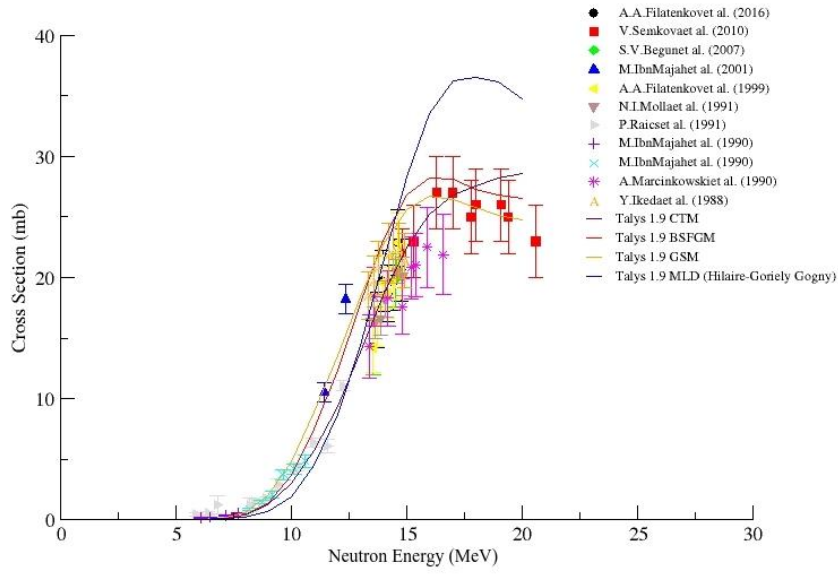


(b)

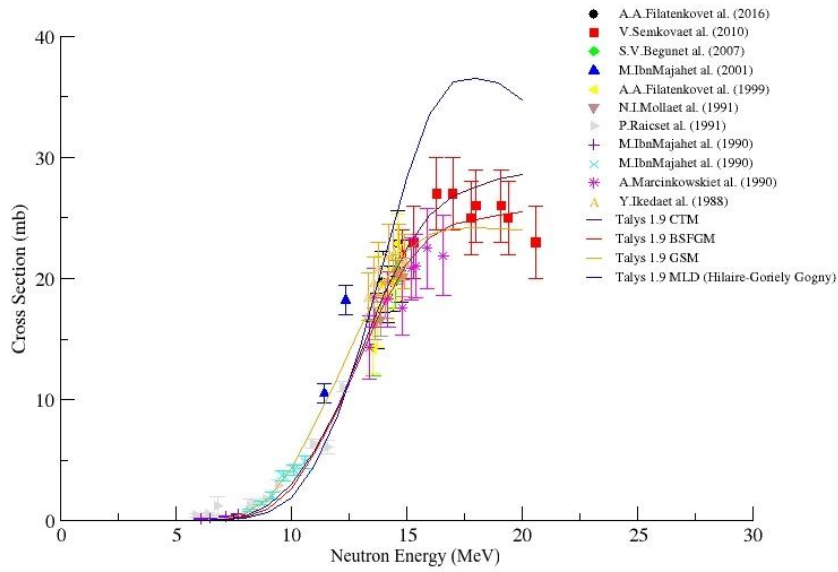
**Figure 17.** The assumptions of all 4 models for the cross-section of the reaction  $^{91}\text{Zr}(n,p)$  calculated using (a) the default value and (b) the best value of level density parameter value, and compared with the experimental data obtained from EXFOR (<https://www-nds.iaea.org>).

**Table 17.** The default and best value of level density parameter for the reaction  $^{91}\text{Zr}(n,p)$ .

$^{91}\text{Zr}(n,p)$	CTM	BSFGM	GSM	MLD
Default	10.62688	9.80719	9.00790	10.93636
Best Fit	9.03284	7.84575	7.65671	10.93636



(a)



(b)

**Figure 18.** The assumptions of all 4 models for the cross-section of the reaction  $^{92}\text{Zr}(n,p)$  calculated using (a) the default value and (b) the best value of level density parameter value, and compared with the experimental data obtained from EXFOR (<https://www-nds.iaea.org>).

**Table 18.** The default and best value of level density parameter for the reaction  $^{92}\text{Zr}(n,p)$ .

$^{92}\text{Zr}(n,p)$	CTM	BSFGM	GSM	MLD
Default	11.51799	9.78980	9.90038	12.12921
Best Fit	11.51799	10.27929	10.39539	12.12921

## CONFLICT OF INTEREST

The author stated that there are no conflicts of interest regarding the publication of this article.

## REFERENCES

- [1] Zinkle SJ and Busby JT. Structural materials for fission & fusion energy, *Materials Today*, vol. 12, Nov. 2009, no. 11. pp. 12–19, , doi: 10.1016/S1369-7021(09)70294-9.
- [2] Motta AT, Couet A and Comstock RJ. Corrosion of Zirconium Alloys used for Nuclear Fuel Cladding, *Annu. Rev. Mater. Res.* 2015, vol. 45, no. 1, pp. 311–343, doi: 10.1146/annurev-matsci-070214-020951.
- [3] Kakiuchi K, Ohira K, Itagaki N, Otsuka Y, Ishii Y and Miyazaki A. Irradiated behavior at high burnup for hifi alloy. *J. Nucl. Sci. Technol.*, 2006; vol. 43, no. 9, pp. 1031–1036, doi: 10.1080/18811248.2006.9711192.
- [4] Parashari S, Mukherjee S, Vansola V, Makwana R, Singh NL and Pandey B. Investigation of (n, p), (n, 2n) reaction cross sections for Sn isotopes for fusion reactor applications. *Appl. Radiat. Isot.*, 2018; vol. 133, pp. 31–37, doi: 10.1016/j.apradiso.2017.12.003.
- [5] Sarpün IH, Aydin A and Pekdoğan H. Determination of the effects of nuclear level density parameters on photofission cross sections of <sup>235</sup>U up to 20 MeV. *EPJ Web Conf.*, vol. 146, pp. 2016–2018, 2017, doi: 10.1051/epjconf/201714605015.
- [6] Aydin A, Pekdoğan H, Kaplan A, Sarpün IH, Tel E and Demir B. Comparison of Level Density Models for the <sup>60,61,62,64</sup>Ni(p, n) Reactions of Structural Fusion Material Nickel from Threshold to 30 MeV. *J. Fusion Energy*, Oct. 2015; vol. 34, no. 5, pp. 1105–1108, doi: 10.1007/s10894-015-9927-2.
- [7] Özdoğan H, Şekerçi M, Sarpün H and Kaplan A. Investigation of level density parameter effects on (p,n) and (p,2n) reaction cross-sections for the fusion structural materials <sup>48</sup>Ti, <sup>63</sup>Cu and <sup>90</sup>Zr. *Appl. Radiat. Isot.*, Oct. 2018; vol. 140, pp. 29–34, doi: 10.1016/j.apradiso.2018.06.013.
- [8] Koning A, Hilaire S and Goriely S. *Talys-1.9: A nuclear reaction program manual*, p. 781, 2017.
- [9] Koning AJ, Hilaire S and Goriely S. Global and local level density models. *Nucl. Phys. A*, 2008; vol. 810, no. 1–4, pp. 13–76, doi: 10.1016/j.nuclphysa.2008.06.005.
- [10] Gilbert A and Cameron AGW. A Composite Nuclear-Level Density Formula with Shell Corrections. *Can J Phys*, Aug. 1965; vol. 43, no. 8, pp. 1446–1496, doi: 10.1139/p65-139.
- [11] Grossjean MK and Feldmeier H. Level density of a Fermi gas with pairing interactions. *Nucl. Phys. A*, Oct. 1985; vol. 444, no. 1, pp. 113–132, doi: 10.1016/0375-9474(85)90294-5.
- [12] Demetriou P and Goriely S. Microscopic nuclear level densities for practical applications. *Nucl. Phys. A*, Dec. 2001; vol. 695, no. 1–4, pp. 95–108, doi: 10.1016/S0375-9474(01)01095-8.
- [13] Dilg W, Schantl W, Vonach H and Uhl M. Level density parameters for the back-shifted fermi

- gas model in the mass range 40 &lt; A &lt; 250. Nucl. Phys. A, Dec. 1973; vol. 217, no. 2, pp. 269–298, doi: 10.1016/0375-9474(73)90196-6.
- [14] Ignatyuk AV, Smirenkin GN and Tishin AS. Phenomenological description of energy dependence of the level density parameter. *Yad. Fiz.*, vol. 21, no. 3, pp. 485–490, 1975, Accessed: Dec. 13, 2019. [Online]. Available: [https://inis.iaea.org/search/search.aspx?orig\\_q=RN:6208426](https://inis.iaea.org/search/search.aspx?orig_q=RN:6208426).
- [15] Baba H. A shell-model nuclear level density. *Nucl. Physics, Sect. A*, 1970; vol. 159, no. 2, pp. 625–641, doi: 10.1016/0375-9474(70)90862-6.
- [16] Goriely S, Hilaire S and Koning AJ, Improved microscopic nuclear level densities within the Hartree-Fock-Bogoliubov plus combinatorial method, *Phys. Rev. C - Nucl. Phys.*, vol. 78, no. 6, p. 064307, Dec. 2008, doi: 10.1103/PhysRevC.78.064307.
- [17] Hilaire S, Girod M, Goriely S and Koning AJ. Temperature-dependent combinatorial level densities with the D1M Gogny force. *Phys. Rev. C - Nucl. Phys.*, 2012; vol. 86, no. 6, p. 064317, Dec. doi: 10.1103/PhysRevC.86.064317.
- [18] Goriely S, Hilaire S, Girod M and Péru S. First Gogny-Hartree-Fock-Bogoliubov nuclear mass model. *Phys. Rev. Lett.*, Jun. 2009; vol. 102, no. 24, doi: 10.1103/PhysRevLett.102.242501.